Inorganic Chemistry

Article

pubs.acs.org/IC

Rapid Ni, Zn, and Cu Ion-Promoted Alcoholysis of *N,N*-Bis(2-picolyl)- and *N,N*-Bis((1*H*-benzimidazol-2-yl)methyl)-*p*-nitrobenzamides in Methanol and Ethanol

Mark A. R. Raycroft, Luana Cimpean, Alexei A. Neverov, and R. Stan Brown*

Department of Chemistry, Queen's University, 90 Bader Lane, Kingston, Ontario, Canada, K7L 3N6

Supporting Information

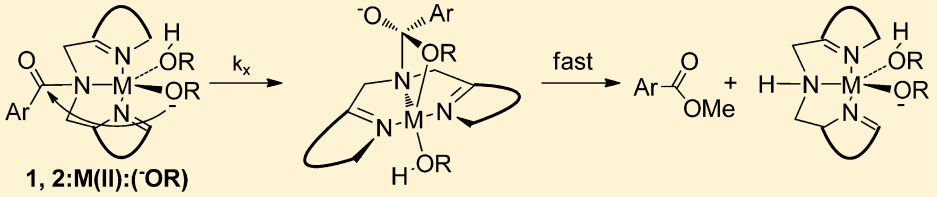

ABSTRACT: The methanolysis and ethanolysis of the Ni(II), Zn(II), and Cu(II) complexes of *N,N*-bis(2-picolyl)-*p*-nitrobenzamide (**1**) and *N,N*-bis((1*H*-benzimidazol-2-yl)methyl)-*p*-nitrobenzamide (**2**) were studied under pH-controlled conditions at 25 °C. Details of the mechanism were obtained from plots of the k_{obs} values for the reaction under pseudo-first-order conditions as a function of $[M^{2+}]$. Such plots give saturation kinetics for the Cu(II)-promoted reactions of **1** and **2** in both solvents, the Zn(II)-promoted reaction of **1** in methanol, and the Zn(II)- and Ni(II)-promoted reactions of **2** in methanol and ethanol. Logs of the maximal observed rate constants obtained from the latter plots, (k_{obs}^{max}), when plotted versus $_{s}^{s}$pH, are curved downward only for the Cu(II) complexes of **1** and **2** in both solvents and the Zn(II) complex of **1** in methanol. Despite differences in the metal-binding abilities and pK_a values for formation of the active form, there is a common reaction mechanism, with the active form being **1**:M(II):($^-$OR) and **2**:M(II):($^-$OR), where M(II):($^-$OR) is the metal-bound alkoxide. The acceleration provided by the metal ion is substantial, being 10^{14}–10^{19} relative to the k_2^{OMe} value for the alkoxide-promoted alcoholysis of the uncomplexed amide.

1.0. INTRODUCTION

The ways by which metal ions promote acyl and phosphoryl transfer reactions include: (a) Lewis acid activation of the substrate; (b) intramolecular delivery of a metal-coordinated lyoxide nucleophile to an activated C═X or P═X unit, where X = O or S; (c) electrostatic stabilization of the transforming activated complex; and (d) electrophilic assistance of the departure of the leaving group (leaving group assistance, LGA).[1−3] The latter role is particularly important for substrates having poor leaving groups with high pK_a values for their conjugate acids such as amides and phosphate- or carboxylate-esters with scissile alkoxy groups. The catalytic cleavage of amides promoted by small molecules presents a stringent challenge due to the amide's inherent resonance stability, which retards nucleophilic addition to the C═O unit, and to poor leaving group ability of the amide anion, which hinders the breakdown of the tetrahedral addition intermediates.[4] The latter case typifies departure of a poor leaving group that is facilitated by protonation or coordination to a metal ion prior to, or concurrent with, its departure.

The catalytic mechanisms of several peptidase enzymes that employ transition metal ions in their active sites have been discussed in the above terms.[5,6] Nature uses Ni(II) ions in the enzyme urease to cleave urea[7] and Zn(II) ions in metallopeptidases like thermolysin and carboxypeptidase[8] to cleave amide bonds in peptides. Considering how effective the metal ions in these metallo-enzymes are, it is surprising that there are only a few small molecule systems capable of cleaving carboxamides[9−11] unless the amide leaving group is activated in some way. Such modes of activation include the release of strain or internal stabilization of the departing amide via resonance, which facilitates departure from the tetrahedral addition intermediates, thus obviating the need for stabilization through LGA.

Metal ion-promoted LGA seems to be an extremely effective but not-often-observed phenomenon in small molecule examples unless there is some special structural character that renders metal ion coordination to the amidic N possible. An interesting example first described by Houghton and Puttner,[12] and subsequently by the groups of Alsfasser[13,14] and Bannwarth,[15] concerned the Cu(II)-promoted methanolysis of N-acyl derivatives of *N,N*-bis(2-picolyl)amine. We have reported detailed kinetic studies of the latter process[16,17] with $_{s}^{s}$pH control in methanol,[18] and show that the reaction elicits a trifunctional role for the Cu(II) that involves its pre-equilibrium coordination to, or close to, the amidic N, subsequent intramolecular attack of a Cu(II)-coordinated methoxide on the C═O, and Cu(II)-assisted C−N cleavage. The catalytically active form of the Cu(II):bis(2-picolyl)acetamide complex

Received: November 20, 2013
Published: February 3, 2014

   dx.doi.org/10.1021/ic4028755 | *Inorg. Chem.* 2014, 53, 2211−2221

involves a substrate-coordinated Cu(II):($^{-}OCH_3$) formed by acid dissociation of the Cu(II):($HOCH_3$), which has a $^{s}_{s}pK_a$ of ≤6.5 in methanol. The catalytic effect of the Cu(II) ion in this solvolysis is quantified to be at least 10^{16} times faster than the rate constant for methoxide attack on *N,N*-bis(2-picolyl)-*p*-nitrobenzamide (**1**).[17] This suggests that, under optimized conditions, man-made catalysts employing metal ion-promoted LGA might rival the rates for peptide (amide) cleavage achievable by enzymes.

The previous studies on the metal ion promoted methanolysis of *N,N*-bis(2-picolyl)-carboxamides[12−15] were performed mostly with Cu(II) salts, but a recent report[15b] discloses that other metal salts, including $FeCl_3$, $NiCl_2$, $Fe(OTf)_3$, AgOTf, and $Zn(OTf)_2$ facilitate the cleavage of *N,N*-bis(2-picolyl)amides in methanol. These experiments were not $^{s}_{s}$pH controlled, making it difficult to ascertain the relative reactivity of each metal ion under conditions where their speciation was unknown. The importance of the M(II)- or M(III)-methoxides for catalytic efficacy in these metal ion-promoted cleavage reactions prompted us to undertake a more detailed kinetic study of the solvolytic cleavage of *N,N*-bis(2-picolyl)-*p*-nitrobenzamide (**1**) in methanol and ethanol promoted by Ni(II), Zn(II), and Cu(II) under $^{s}_{s}$pH-controlled conditions. In addition, we have completed an analogous study of the metal ion-promoted cleavage of *N,N*-bis((1H-benzimidazol-2-yl)methyl)-*p*-nitrobenzamide (**2**) where the amine ligand is readily available from an easily scalable, one-step reaction.[19]

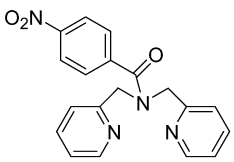

1

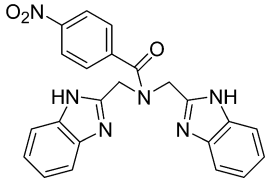

2

2.0. EXPERIMENTAL SECTION

2.1. Materials. Methanol (99.8%, anhydrous) and acetonitrile (99.8%, anhydrous) were purchased from EMD Chemicals. Absolute ethanol (anhydrous, degassed, stored under argon, and freshly dispensed for kinetic experiments) was purchased from Commercial Alcohols (GreenField Ethanol Inc.). Acetone (99.5%) was purchased from ACP Chemicals. Trifluoromethanesulfonic acid (HOTf, ≥99%), 1,2-phenylenediamine (99.5%), *p*-nitrobenzoyl chloride (98%), 2-bromo-6-methylpyridine (98%), 2-picoline (98%), 2,6-lutidine (≥99%), *N*-ethylmorpholine (99%), *N*-methylpiperidine (99%), zinc trifluoromethanesulfonate (98%), and sodium ethoxide (21 wt % in denatured ethanol) were purchased from Aldrich, and 2-methoxy-6-methylpyridine (98%) was purchased from AK Scientific. 2,4,6-Collidine (98%) was purchased from BDH Laboratory Reagents. Iminodiacetic acid (98%) was purchased from Alfa Aesar. Potassium carbonate (99%), ethylene glycol (≥99%), and sodium methoxide (0.5 M solution in methanol) were purchased from Sigma-Aldrich. Copper(II) trifluoromethanesulfonate (98%) was obtained from TCI America Laboratory Chemicals. Nickel(II) perchlorate hexahydrate (reagent grade) was purchased from GFS Chemicals.

2.2. General Methods. ^{1}H NMR spectra were determined at 400 MHz and ^{13}C NMR spectra at 100.58 MHz. High-resolution mass spectra (HRMS) were determined by electron impact time of flight (EI-TOF). All $CH_3OH_2^+$ and $CH_3CH_2OH_2^+$ concentrations were determined potentiometrically using a combination glass Fisher Scientific Accumet electrode (model no. 13-620-292) calibrated with certified standard aqueous buffers (pH 4.00 and 10.00) as described previously.[20] The $^{s}_{s}$pH values in methanol were determined by subtracting a correction constant of −2.24[18] from the electrode readings, and the autoprotolysis constant for methanol was taken to be $10^{-16.77}$ M^2. The $^{s}_{s}$pH values in ethanol were determined by subtracting a correction constant of −2.54[18] from the electrode readings, and the autoprotolysis constant for ethanol was taken to be $10^{-19.1}$ M^2. The $^{s}_{s}$pH values for the kinetic experiments were measured at the end of the reactions to avoid the effect of KCl leaching from the electrode.

2.3. Synthesis. *N,N-bis(2-picolyl)-p-nitrobenzamide (1).*[17] This was synthesized and characterized as previously reported. *N,N*-bis((1*H*-benzimidazol-2-yl)methyl)-*p*-nitrobenzamide (**2**) was prepared by acylation with *p*-nitrobenzoyl chloride, modeled on that for the acylation by acetyl chloride.[21] In a 50-mL round-bottom flask, *N,N*-bis((1*H*-benzimidazol-2-yl)methyl)amine (573.3 mg, 2.067 mmol) was dissolved in acetone (15 mL) by stirring for 10 min. Excess potassium carbonate was added, and the mixture was stirred for an additional 10 min at RT and then placed in an ice−water bath. In a separate vial, *p*-nitrobenzoyl chloride (728.3 mg, 3.924 mmol) was dissolved in acetone (5 mL), cooled in an ice−water bath, and then added dropwise to the reaction mixture. The solution was left to stir and warm to RT overnight. The resulting orange solid was vacuum-filtered and dried under vacuum. Column chromatographic separation was carried out using a medium pressure liquid chromatography (MPLC) apparatus (silica stationary phase, EtOAc/MeOH mobile phase). The product was obtained as a yellow solid in 65.8% yield (580.0 mg, 1.360 mmol).

HRMS (EI-TOF): calculated for $C_{23}H_{18}N_6O_3$ 426.1440 amu, found 426.1457 amu. ^{1}H NMR (400 MHz, CD_3OD, 25 °C) δ 7.98 (m, 2H; A^{phenyl}), 7.63 (m, 2H; B^{phenyl}), 7.52 (m, 4H; $A^{benzimidazolyl}$), 7.18 (bm, 4H; $B^{benzimidazolyl}$), 5.06 (bs, 2H), 4.85 (bs, 2H). ^{13}C NMR (100.58 MHz, CD_3OD, 25 °C) δ 172.5, [152.0, 151.7], 150.0, 142.2, 139.6 (br), 129.3, 124.8, [124.0, 123.9], 116.0 (br), [49.5 (br), 46.0 (br)] (square brackets are used to designate pairs of ^{13}C signals that are related by rotation). Both ^{1}H and ^{13}C NMR spectra can be found in Supporting Information (Figures 1S−5S). Ultraviolet−visible (UV−vis) absorbance spectrum in anhydrous methanol: $\varepsilon_{274\ nm}$ = (26.3 ± 0.3) × 10^3 M^{-1} cm^{-1}, $\varepsilon_{281\ nm}$ = (24.7 ± 0.3) × 10^3 M^{-1} cm^{-1}. Melting point: 202.8 °C (dec).

2.4. General UV−vis Kinetics. All kinetic experiments were conducted using a UV−vis spectrophotometer with the cell compartment thermostatted at 25.0 ± 0.1 °C. The reactions were conducted in the presence of buffers composed of various ratios of amine (2-methoxy-6-methylpyridine $^{s}_{s}pH^{MeOH}$ = 5.0, $^{s}_{s}pH^{EtOH}$ = 4.2−4.5; 2-picoline $^{s}_{s}pH^{MeOH}$ = 5.3−6.6, $^{s}_{s}pH^{EtOH}$ = 5.0−6.5; 2,6-lutidine $^{s}_{s}pH^{EtOH}$ = 5.9−6.8; 2,4,6-collidine $^{s}_{s}pH^{MeOH}$ = 7.0−8.0, $^{s}_{s}pH^{EtOH}$ = 7.0−7.9; *N*-ethylmorpholine $^{s}_{s}pH^{MeOH}$ = 8.5−9.2; *N*-methylpiperidine $^{s}_{s}pH^{MeOH}$ = 9.8−10.5) and HOTf to maintain the $^{s}_{s}$pH in methanol or ethanol. The upper limits on $^{s}_{s}$pH were determined by the $^{s}_{s}pK_a$ values for the acid dissociation of the alcohol solvates of Ni(II), Zn(II), and Cu(II) in methanol and ethanol (from their potentiometric titration profiles[22]) to avoid oligomerization of metal ion alkoxides. A typical kinetic experiment for the alcoholysis of **1** involved preparation of an alcohol solution containing buffer (10 mM), **1** (0.05 mM or 0.5 mM), and M^{2+} (0.1−4.0 mM as the perchlorate or triflate) in a 1 cm path length quartz cuvette. The reaction was initiated by the addition of an aliquot of the M^{2+} stock solution to the buffered solution containing **1** to achieve the desired concentrations of the reaction components at a final volume of 2.5 mL. A typical kinetic experiment for the alcoholysis of **2** involved preparation of an alcohol solution containing buffer (2 mM), **2** (0.02 mM), and M^{2+} (0.02−0.2 mM as the perchlorate or triflate) in a 1 cm path length quartz cuvette. The reaction was initiated by the addition of an aliquot of the M^{2+} stock solution to the buffered solution containing **2** to achieve the desired concentrations of the reaction components at a final volume of 2.5 mL. Experiments were performed in duplicate, and the abs versus time traces for the disappearance of the starting complex were fit with a standard first-order exponential equation to a minimum of 5 half-life times to obtain the k_{obs} values.

The analogous Ni^{2+}, Cu^{2+}, and Zn^{2+} catalyzed methanolyses and ethanolyses of **1** or **2** were conducted under $^{s}_{s}$pH-controlled conditions using various buffers, and were monitored by observing, with UV−vis

dx.doi.org/10.1021/ic4028755 | Inorg. Chem. 2014, 53, 2211−2221

spectrophotometry at 25.0 °C, the rate of loss of complex or formation of M(II)-coordinated amine at various wavelengths. The details for each metal ion and complex are described in Supporting Information.

2.5. Product Analyses. The methanolysis and ethanolysis of M(II):**1** and M(II):**2** (M(II) = Ni(II), Zn(II), Cu(II)) were conducted at higher concentration in ROH (R = CH_3, CH_3CH_2), where $[M^{2+}]$ = 4 mM, [**1** or **2**] = 2 mM, [NaOR] = 2 mM. After completion of the reaction (assessed by UV−vis spectroscopy), the solvent was rotary-evaporated, and the residue was dissolved in CD_3OD, after which the ^{1}H NMR spectrum (400 MHz) was collected. In the cases of Ni(II) and Cu(II), the only observable product was the corresponding methyl or ethyl benzoate. The Ni(II) or Cu(II) complex of *N*,*N*-bis(2-picolyl)amine or *N*,*N*-bis((1*H*-benzimidazol-2-yl)methyl)amine was not observed by ^{1}H NMR due to Ni(II)- or Cu(II)-induced paramagnetic broadening. In the case of Zn(II), sharp signals corresponding to the methyl or ethyl benzoate were observed as well as broadened signals corresponding to the Zn(II) complex of *N*,*N*-bis(2-picolyl)amine or *N*,*N*-bis((1*H*-benzimidazol-2-yl)methyl)-amine.

3.0. RESULTS

3.1. M(II)-Promoted Methanolysis of 1. *3.1.1. Kinetics of the Ni(II)-Promoted Methanolysis of 1.* The Ni(II)-promoted methanolysis of 5×10^{-5} M **1** was studied from $7.2 \leq {}^{s}_{s}\text{pH} \leq 10.5$ under buffered conditions in the presence of variable but excess $[Ni(ClO_4)_2]$. The effect of buffer inhibition was assessed at each ${}^{s}_{s}$pH by monitoring the $[M^{2+}]$-dependence at two concentrations (10 mM and 20 mM) of buffer; in all cases the two $[M^{2+}]$-dependent second-order rate constants were either very close to or within experimental error. As the effect of buffer was found to be insignificant, only the data at 10 mM buffer are reported. The upper limit on the ${}^{s}_{s}$pH range was limited by the ${}^{s}_{s}pK_a$ for the acid dissociation of the solvated metal in methanol $(Ni(II)_s{:}(HOCH_3) + HOCH_3 \rightleftharpoons Ni(II)_s{:}(^{-}OCH_3) + H_2O^{+}CH_3$ (${}^{s}_{s}pK_a$ = 11.24)[22]) to maintain the speciation of Ni(II) reasonably constant in its neutral solvated form. Saturation binding of Ni(II) with **1** was not observed, as evidenced by linear dependencies of the k_{obs} values on $[Ni^{2+}]$ at each ${}^{s}_{s}$pH over the range of $0 < [Ni(ClO_4)_2] \leq 4.0$ mM; a representative example is shown in Figure 1.

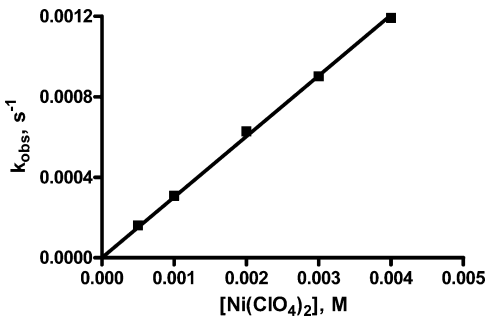

Figure 1. Plot of k_{obs} for the cleavage of 5×10^{-5} M **1** vs $[Ni(ClO_4)_2]$ buffered at ${}^{s}_{s}$pH 8.5 (10 mM N-ethylmorpholine, 5 mM HOTf) in anhydrous methanol at 25 °C. The data are fitted to a linear regression computing $k_2 = (0.301 \pm 0.003)$ M^{-1} s^{-1}.

The lack of saturation kinetics for the decomposition of **1** with increasing $[Ni^{2+}]$ signifies that the metal ion is far from being completely bound under the experimental conditions, a conclusion supported by ^{1}H NMR experiments where the addition of 1 equiv of $Ni(ClO_4)_2$ resulted in only a small perturbation of the ^{1}H NMR spectrum of **1**. The second-order rate constants (k_2) for the metal-ion promoted reactions are given as the gradients of the k_{obs} versus $[Ni(ClO_4)_2]$ plots at each ${}^{s}_{s}$pH. Shown in Figure 6S (Supporting Information) is a plot of $\log(k_2)$ versus ${}^{s}_{s}$pH, which is linear with a slope of 0.89 ± 0.03, which is considered as experimental support that one methoxide is involved in the transition state (TS) for the reaction, probably by way of its being coordinated to the Ni(II).

3.1.2. Kinetics of the Zn(II)-promoted methanolysis of 1. The Zn(II)-promoted methanolysis of **1** was studied from $8.5 \leq {}^{s}_{s}\text{pH} \leq 10.0$ under buffered conditions in the presence of excess $Zn(OTf)_2$. Buffer dependence studies were conducted as described above for Ni(II), and the effect of buffer was found to be insignificant. As is the case of Ni(II)-promoted cleavage of **1**, the k_{obs} values depend linearly on metal ion concentration, this time over a narrower concentration range of 0−2 mM of $Zn(OTf)_2$. As has been confirmed by experiments with varying concentrations of **1** at the higher ${}^{s}_{s}$pH values, an observed downward curvature of the concentration/rate profile at $[Zn(OTf)_2] > 2$ mM is not due to saturation binding with **1**, but is rather due to dimerization or oligomerization of the $Zn(II){:}(^{-}OCH_3)$ species. Given in Figure 7S (Supporting Information) is a plot of $\log(k_2)$ versus ${}^{s}_{s}$pH, which is linear with a slope of 0.97 ± 0.05.

3.1.3. Kinetics of the Cu(II)-Promoted Methanolysis of 1. Our previous study[17] of the Cu(II)-promoted methanolysis of **1** was expanded to encompass a broader ${}^{s}_{s}$pH range of 5.0−8.0 under buffered conditions in the presence of excess $Cu(OTf)_2$ (to ensure complete binding to **1**). All k_{obs} values were corrected for inhibitory effects of buffer and excess $Cu(OTf)_2$, and a plot of the log of the corrected rate constants ($\log(k_{obs}^{corr})$) versus ${}^{s}_{s}$pH is given in Figure 2. NLLSQ fitting of the data to eq 1 yielded a kinetic ${}^{s}_{s}pK_a$ value of 5.79 ± 0.07 and a maximum rate constant (k_{max}) of $(5.7 \pm 0.4) \times 10^{-3}$ s^{-1}.

$$\log(k_{obs}) = \log\left(\frac{k_{max} \times {}^{s}_{s}K_a}{{}^{s}_{s}K_a + [H^+]}\right) \quad (1)$$

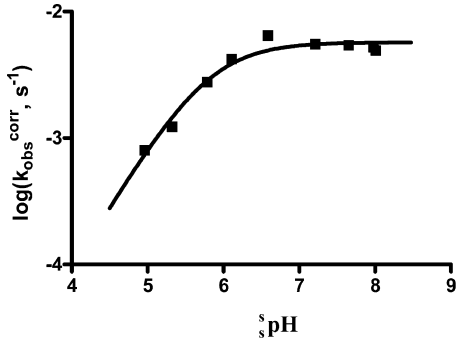

Figure 2. A plot of $\log(k_{obs}^{corr})$ vs ${}^{s}_{s}$pH for the cleavage of **1**:Cu(II) (0.5 mM each of Cu(II) and **1** and corrected for buffer and excess Cu^{2+} effects) in anhydrous methanol under buffered conditions at 25 °C. The data are NLLSQ fit to eq 1 to give a kinetic ${}^{s}_{s}pK_a$ of 5.79 ± 0.07 and a maximum rate constant (k_{max}) of $(5.7 \pm 0.4) \times 10^{-3}$ s^{-1}; r^2 = 0.9666.

3.2. M(II)-Promoted Ethanolysis of 1. *3.2.1. Kinetics of the Ni(II)-Promoted Ethanolysis of 1.* Although saturation kinetics are not observed with Ni^{2+} or Zn^{2+} in methanol, the favored process for the reaction of other divalent metal ion complexes should proceed via formation of the essential intermediate, **1**:M(II):$(^{-}OCH_3)$, with the metal ion bound to the two pyridines and an alkoxide as in Scheme 1. Earlier

dx.doi.org/10.1021/ic4028755 | Inorg. Chem. 2014, 53, 2211−2221

Scheme 1. Proposed Reaction Scheme for the M(II)-Promoted Solvolysis of 1 (R = Me, Et)

studies[23] have shown that a change in medium to one with a lower dielectric constant, such as from methanol to ethanol (ϵ_r = 31.5 and 24.3),[24] greatly increases the binding of anionic substrates and metal ion complexes, and a similar phenomenon should exist with the binding of M^{2+} and **1**.

The Ni(II)-promoted ethanolysis of 5 × 10^{-5} M **1** was studied from 5.9 ≤ $^{s}_{s}$pH ≤ 7.9[25] under buffered conditions in the presence of excess $Ni(ClO_4)_2$. At all $^{s}_{s}$pH values in this range the plots of k_{obs} versus $[Ni(ClO_4)_2]$ exhibit a downward curvature consistent with a saturation binding process; a representative example is shown in Figure 3. NLLSQ fitting of

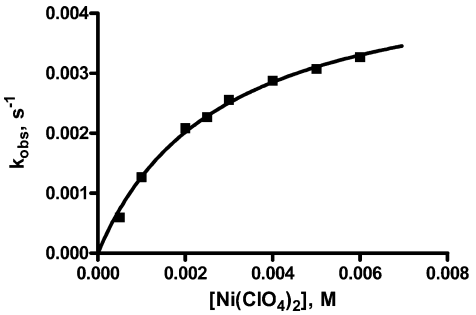

Figure 3. Plot of k_{obs} for the cleavage of 5 × 10^{-5} M **1** vs $[Ni(ClO_4)_2]$ buffered at $^{s}_{s}$pH 6.7 (10 mM 2,6-lutidine, 5 mM HOTf) in anhydrous ethanol at 25 °C. The data were fitted to a standard one-site binding model to give K_b = (360 ± 30) M^{-1} and k_{obs}^{max} = (4.8 ± 0.2) × 10^{-3} s^{-1}; r^2 = 0.9953.

the data to a standard one-site binding model gives the metal binding constant (K_b) and maximal observed rate constant (k_{obs}^{max}) at each $^{s}_{s}$pH. Additional kinetic experiments using increasing concentrations of tetrabutylammonium perchlorate (0–20 mM) demonstrated that there is no significant effect of additional perchlorate anions on the rate of the reaction. The linear plot of log(k_{obs}^{max}) versus $^{s}_{s}$pH shown in Figure 4 has a slope of 0.89 ± 0.06.

Considering the error limits and the fact that k_{obs}^{max} and K_b are heavily correlated, second-order rate constants for the metal ion-catalyzed reaction at each $^{s}_{s}$pH (k_2) were calculated as $k_{obs}^{max}K_b$. Figure 4 also presents a plot of log(k_2) versus $^{s}_{s}$pH that exhibits a linear dependence on $[^{-}OCH_3]$ with a gradient of 0.93 ± 0.09.

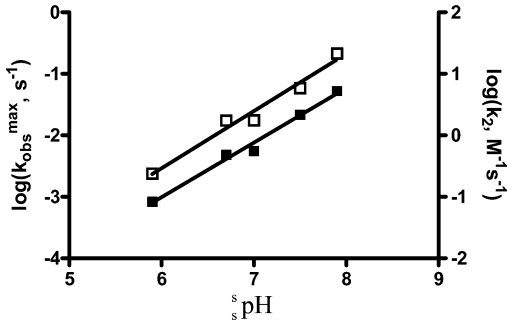

Figure 4. Plots of log(k_{obs}^{max}) (■) and log(k_2) (□) for the Ni(II)-promoted cleavage of **1** vs $^{s}_{s}$pH in anhydrous ethanol under buffered conditions (10 mM amine, various concentrations of HOTf) at 25 °C. The lines through the data are generated from linear regressions to provide slopes of 0.89 ± 0.06 (r^2 = 0.9864) and 0.93 ± 0.09 (r^2 = 0.9731), respectively.

3.2.2. Kinetics of the Zn(II)-Promoted Ethanolysis of 1. The Zn(II)-promoted ethanolysis of 5 × 10^{-5} M **1** was studied from 6.2 ≤ $^{s}_{s}$pH ≤ 7.2 under buffered conditions in the presence of excess $Zn(OTf)_2$. Over this range the plots of k_{obs} versus $[Zn(OTf)_2]$ exhibit a slight downward curvature indicative of a weak, yet quantifiable, binding between Zn(II) and **1**. Fits of the k_{obs} versus $[Zn^{2+}]$ data to a standard 1:1 binding expression gave the binding constants (K_b) and maximum rate constants (k_{obs}^{max}) for the decomposition of the metal bound complex at each $^{s}_{s}$pH. The plot of log(k_{obs}^{max}) versus $^{s}_{s}$pH in Figure 5 has a

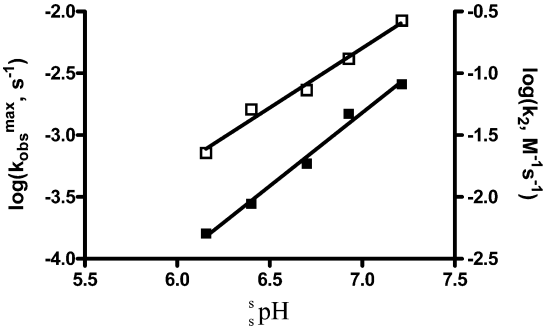

Figure 5. Plots of log(k_{obs}^{max}) (■) and log(k_2) (□) for the Zn(II)-promoted cleavage of 5 × 10^{-5} M **1** vs $^{s}_{s}$pH in anhydrous ethanol under buffered conditions (10 mM amine, various concentrations of HOTf) at 25 °C. The lines through the data are generated from linear regressions to provide slopes of 1.19 ± 0.07 (r^2 = 0.9890) and 0.96 ± 0.07 (r^2 = 0.9833), respectively.

slope of 1.19 ± 0.07. Second-order rate constants for the reaction of Zn(II)-promoted reaction of **1** at each $^{s}_{s}$pH were calculated as the product of the k_{obs}^{max} and K_b values. The plot of log(k_2) versus $^{s}_{s}$pH (Figure 5) gives a straight line with a gradient of 0.96 ± 0.07.

3.2.3. Kinetics of the Cu(II)-Promoted Ethanolysis of 1. The Cu(II)-promoted ethanolysis of 5 × 10^{-4} M **1** was studied from 3.3 ≤ $^{s}_{s}$pH ≤ 7.6 under buffered conditions in the presence of excess $Cu(OTf)_2$ (to ensure complete binding to **1**). All k_{obs} values were corrected for inhibitory buffer and excess $Cu(OTf)_2$ effects, and the k_{obs}^{corr} was plotted in logarithmic form as a function of $^{s}_{s}$pH (Figure 13S, Supporting Information). NLLSQ fits of these data to eq 1 yield a kinetic $^{s}_{s}pK_a$ of 5.4 ± 0.1 and a maximum rate constant (k_{max}) of (9 ± 1) × 10^{-3} s^{-1}.

dx.doi.org/10.1021/ic4028755 | Inorg. Chem. 2014, 53, 2211–2221

3.3. M(II)-Promoted Methanolysis of 2. *3.3.1. Kinetics of the Ni(II)-Promoted Methanolysis of 2.* The Ni(II)-promoted methanolysis of 2×10^{-5} M **2** was studied from $7.2 \leq {}^{s}_{s}\text{pH} \leq 10.2$ in the presence of variable concentrations of excess $Ni(ClO_4)_2$. Unlike the Ni(II)-catalyzed cleavage of **1** in methanol, a plot of the k_{obs} values for the cleavage of **2** versus $[Ni^{2+}]$ in ethanol exhibits saturation metal binding, which was analyzed to give K_b and k_{obs}^{max} values. The linear plot of $\log(k_{obs}^{max})$ versus ${}^{s}_{s}\text{pH}$ shown in Figure 14S (Supporting Information) has a slope of 0.94 ± 0.02. Second-order rate constants were calculated from the k_{obs}^{max} and K_b values and plotted as $\log(k_2)$ versus ${}^{s}_{s}\text{pH}$ (Figure 15S Supporting Information), exhibiting a linear dependence with a gradient of 0.98 ± 0.05.

3.3.2. Kinetics of the Zn(II)-Promoted Methanolysis of 2. The Zn(II)-promoted methanolysis of 2×10^{-5} M **2** was studied from $7.0 \leq {}^{s}_{s}\text{pH} \leq 9.2$ in the presence of variable concentrations of excess $Zn(OTf)_2$. The plots of the k_{obs} values for the cleavage of **2** versus $[Zn^{2+}]$ in ethanol exhibit saturation binding. NLLSQ fitting of the $\log(k_{obs}^{max})$ and ${}^{s}_{s}\text{pH}$ data (Figure 6) gives a kinetic ${}^{s}_{s}\text{p}K_a$ of 8.36 ± 0.07 and a maximum rate

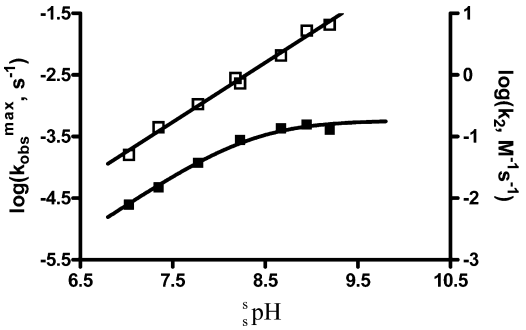

Figure 6. Plots of $\log(k_{obs}^{max})$ (■) and $\log(k_2)$ (□) for the Zn(II)-promoted cleavage of **2** vs ${}^{s}_{s}\text{pH}$ in anhydrous methanol under buffered conditions (10 mM amine, various concentrations of HOTf) at 25 °C. The ■ data are NLLSQ fitted to eq 1 to give a kinetic ${}^{s}_{s}\text{p}K_a$ of 8.36 ± 0.07 and a maximum rate constant for the decomposition of the **2**:Zn(II):($^{-}OCH_3$) complex (k_{max}) of $(5.8 \pm 0.6) \times 10^{-4}$ s^{-1}; r^2 = 0.9903. The linear regression fit of the □ data has a slope of 0.97 ± 0.04; r^2 = 0.9912.

constant (k_{max}) of $(5.8 \pm 0.6) \times 10^{-4}$ s^{-1}. Second-order rate constants for the metal ion-catalyzed reaction were calculated from the k_{obs}^{max} and K_b values and plotted in the form of $\log(k_2)$ as a function of ${}^{s}_{s}\text{pH}$ (Figure 6), exhibiting a linear dependence with a gradient of 0.97 ± 0.04. Of note in Figure 6 is the fact that the $\log(k_2)$ value is linear above the saturation ${}^{s}_{s}\text{pH}$ for the k_{obs}^{max} plot, suggesting that the binding of the metal ion is strongest when it has an attached methoxide.[26,27]

3.3.3. Kinetics of the Cu(II)-Promoted Methanolysis of 2. The Cu(II)-promoted methanolysis of 2×10^{-5} M **2** was studied from $4 \leq {}^{s}_{s}\text{pH} \leq 8.5$ under buffered conditions. Cu(II) is completely bound to **2** as evidenced by a maximum in the k_{obs} versus $[Cu^{2+}]$ plot at a 1:1 ratio of metal ion to substrate, followed by a slight decrease in cleavage rate with increasing $[Cu(OTf)_2]$. Such a decrease in rate may be attributed to inhibition by triflate ions or to minor changes in ionic strength. The ${}^{s}_{s}\text{pH}$-independent plateau region depicted in Figure 18S, Supporting Information, arises from the decomposition of the **2**:Cu(II):(^{-}OMe) complex, the average of all k_{obs}^{max} values being $(8.0 \pm 0.8) \times 10^{-4}$ s^{-1}.

3.4. M(II)-Promoted Ethanolysis of 2. *3.4.1. Kinetics of the Ni(II)-Promoted Ethanolysis of 2.* The Ni(II)-promoted ethanolysis of 2×10^{-5} M **2** was studied from $5.2 \leq {}^{s}_{s}\text{pH} \leq 8.7$ under buffered conditions and in the presence of variable concentrations of excess $Ni(ClO_4)_2$. The kinetics also indicate saturation binding with increasing $[Ni^{2+}]$, which is analyzed to give a k_{obs}^{max} value at each ${}^{s}_{s}\text{pH}$. The linear plot of $\log(k_{obs}^{max})$ versus ${}^{s}_{s}\text{pH}$ shown in Figure 7 has a slope of 1.11 ± 0.03. Second-order

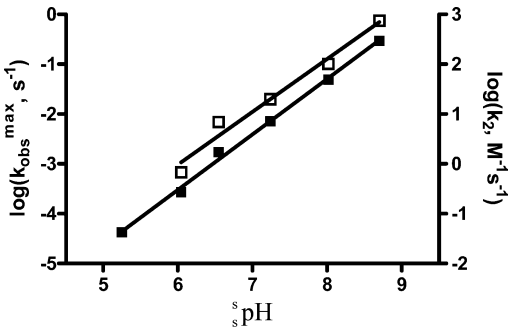

Figure 7. Plots of $\log(k_{obs}^{max})$ (■) and $\log(k_2)$ (□) for the Ni(II)-promoted cleavage of **2** vs ${}^{s}_{s}\text{pH}$ in anhydrous ethanol under buffered conditions (10 mM amine, various concentrations of HOTf) at 25 °C. The lines through the data are generated from linear regressions to provide slopes of 1.11 ± 0.03 (r^2 = 0.9967) and 1.05 ± 0.09 (r^2 = 0.9787), respectively.

rate constants were calculated from k_{obs}^{max} and K_b values and plotted in the form of $\log(k_2)$ as a function of ${}^{s}_{s}\text{pH}$ (Figure 7), exhibiting a linear dependence with a gradient of 1.05 ± 0.09.[28]

3.4.2. Kinetics of the Zn(II)-Promoted Ethanolysis of 2. The Zn(II)-promoted ethanolysis of 2×10^{-5} M **2** was studied from $5.9 \leq {}^{s}_{s}\text{pH} \leq 7.5$ in the presence of three concentrations of excess $Zn(OTf)_2$. The k_{obs} values for the cleavage of **2** exhibit a saturation phenomenon with increasing $[Zn^{2+}]$. The linear plot of $\log(k_{obs}^{max})$ versus ${}^{s}_{s}\text{pH}$ shown in Figure 8 has a slope of 1.00 ±

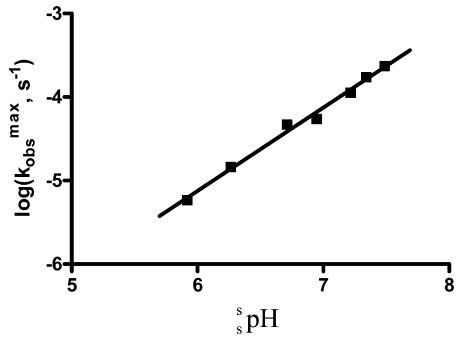

Figure 8. Plot of $\log(k_{obs}^{max})$ for the Zn(II)-promoted cleavage of **2** vs ${}^{s}_{s}\text{pH}$ in anhydrous ethanol under buffered conditions (2 mM amine, various concentrations of HOTf) at 25 °C. The line through the data is generated from a linear regression with a slope of 1.00 ± 0.04; r^2 = 0.9914.

0.04. The second-order rate constants (k_2^{Zn}) were not calculated due to the large uncertainties in the binding constants (K_b), which stem from strong interactions between the metal ion and the substrate.[29] However, generally the kinetically determined K_b values are large, being in the range of 10^5–10^6 M^{-1}, which can only be determined with an appreciable error.

3.4.3. Kinetics of the Cu(II)-Promoted Ethanolysis of 2. The Cu(II)-promoted ethanolysis of 2×10^{-5} M **2** was studied over a narrow range of $6.9 \leq {}^{s}_{s}\text{pH} \leq 7.7$ under buffered conditions where, at 1:1 concentrations, Cu(II) is expected to be

dx.doi.org/10.1021/ic4028755 | Inorg. Chem. 2014, 53, 2211–2221

completely bound to **2** for the same reasons described for the reaction in methanol. The plateau region depicted in Figure 22S, Supporting Information, represents the maximum rate constant (k_{max}) for the unimolecular decomposition of **2**:Cu(II):($^{-}$OEt), the average value being (3.8 ± 0.2) × 10^{-4} s^{-1}.

4.0. DISCUSSION

Previous studies examined the Cu(II)-promoted solvolytic cleavage of *N*,*N*-bis(2-picolyl)amides facilitated by its binding to the amidic nitrogen. These provided evidence for the mechanism shown in Scheme 1 in truncated form, which involves metal ion complexation followed by formation of the metal-bound alkoxide, which then acts as the nucleophile toward the closely positioned C═O. Importantly, in a subsequent step, the Cu(II) acts to assist the departure of the leaving amide group.[16,17] In those studies, the experimental and computational data with *p*-nitro, H, and *p*-OCH_3 substituted benzoyl derivatives supported a mechanism where a Cu(II) ion is bound to the *N*,*N*-bis(2-picolyl)amide unit and positioned so that it permits delivery of a metal-coordinated methoxide nucleophile to the C═O in the rate-limiting TS of the reaction. This proceeds to a tetrahedral intermediate, occupying a shallow minimum on the free-energy surface with the Cu(II) coordinated to both the methoxide and amidic N. Breakdown of the latter is virtually barrierless, involving a Cu(II)-assisted departure of the bis(2-picolyl)amide anion and a loosening of the Cu(II)-OCH_3 bond. Given the shallowness of the potential surface subsequent to formation of the tetrahedral intermediate, the latter is considered to have an insufficient lifetime to exist, so the overall process is termed enforced−concerted.[30] While we have not performed the required computations with all metal ions, substrates, and solvents that form the subject matter in the present study, the overall mechanism is likely similar to rate limiting nucleophilic attack of the metal coordinated alkoxide and subsequent fast, or barrierless, breakdown of an unstable intermediate.

Bannwarth and co-workers[15b] have reported a brief survey of the potential of some other metal ions in a study of what were termed "chelating carboxylic acid amides as robust relay protecting groups of carboxylic acids." The latter study compared the effectiveness of several metal ion salts on the cleavage of *N*,*N*-bis(2-picolyl)-*p*-iodobenzamide in methanol containing a set amount of metal ion for 16 h at room temperature. Because this study was a comparative assessment of the utility of various metal ions under a common condition, there was no determination of the relative constants for metal binding to the substrates, nor was the $^{s}_{s}$pH measured and controlled. Given that the recent mechanistic work[16,17] indicates the lyoxide form of the bound metal complex is important for the Cu(II)-promoted cleavage, the speciation of other analogous metal ion complexes may also be important. In such cases, the complexes may only exhibit their maximal activities when fully bound with metal ion methoxide and these activities may well be far greater than what was reported to be the case at the set condition.[15b]

The observations in the present work indicate all the metal ions are active and suggest that their various behaviors fall into three subsets of a common mechanism encompassed by that shown in Scheme 1. These are controlled by the values of the substrate:M(II) binding constant, K_b, and the substrate:M(II):(HOR) acid dissociation constant, $^{s}_{s}K_a$, leading to formation of the essential substrate:M(II):($^{-}$OR) complex. In a given case one can observe: (1) saturation binding of substrate with metal ion, as well as a low $^{s}_{s}pK_a$ for formation of substrate:M(II):($^{-}$OR) complex; (2) saturation of metal ion binding, but a high enough $^{s}_{s}pK_a$ for proton dissociation from the substrate:M(II):(HOR) complex that the reaction appears first order in ($^{-}$OR) throughout the $^{s}_{s}$pH range investigated; and (3) no saturation of metal binding to substrate, and an observed first order dependence on the reaction rate on both [M^{2+}] and [$^{-}$OR] over the $^{s}_{s}$pH range investigated.

4.1. Ni(II)- and Zn(II)-Promoted Methanolysis of *N*,*N*-Bis(2-picolyl)-*p*-nitrobenzamide (1). Neither metal ion gives evidence of saturation binding to the substrate up to concentrations of 4 mM (Ni^{2+}) or 2 mM (Zn^{2+}). The near unit value of the gradients of the log(k_2) versus $^{s}_{s}$pH plots in Figures 6S and 7S, Supporting Information, is consistent with a first-order dependence of the reaction rate on [$^{-}OCH_3$], as expected for the mechanism in Scheme 1. This is similar to what was previously proposed for the Cu(II)-promoted cleavage of **1**,[17] which involves strong coordination of Cu^{2+} followed by nucleophilic attack by the Cu(II)-coordinated methoxide and metal-assisted departure of the leaving group.[31] Strong binding of Cu^{2+} to **1** was evident from the observation of a downward curvature in the k_{obs} versus [Cu^{2+}] plots, and the plateau in its $^{s}_{s}$pH/log(k^{max}_{obs}) plot above $^{s}_{s}$pH 6 is consistent with the maximal activity being due to unimolecular decomposition of the **1**:Cu(II):($^{-}OCH_3$) form. The weaker binding of Ni(II) and Zn(II) relative to Cu(II) correlates well with their known binding constants with pyridine. For example, the dissociation constant for the complex Ni(II):Pyr_2 in water (1.48 × 10^{-3} M^2; μ = 0.5) is approximately 40 times larger than that for Cu(II):Pyr_2 (4.11 × 10^{-5} M^2; μ = 0.5),[32] while the stability constants of the monopyridine complexes of Ni(II) and Cu(II) are 87 and 398 M^{-1}, respectively, at μ = 0.5.[33] Weaker complexes are formed between Zn(II) and pyridine ligands relative to Ni(II). The dissociation constant for the complex Zn(II):Pyr_2 in water is 7.8 × 10^{-2} M^2 (μ = 0.1) versus 1.48 × 10^{-3} M^2 (μ = 0.5) for Ni(II):Pyr_2[32], while the stability constants for the monopyridine complexes of Zn(II) and Ni(II) are 14 and 87 M^{-1}, respectively.[33]

The strong effect that $^{s}_{s}$pH has on the rate of the Ni(II)-, Zn(II)-, and other metal ion-catalyzed processes[12−15,15b] gives a clear message that the activated complexes contain methoxide, probably bound to the ligand-complexed metal ion prior to the rate-limiting decomposition. In a given case, without confirmation of speciation and $^{s}_{s}$pH control, the overall catalytic effect of different metal ions with different substrates may be understated since the reactions may not have been investigated under conditions where the **1**:M(II):($^{-}OCH_3$) complex is fully formed. Because of the stronger binding of Cu(II), and its acidifying effect on coordinated solvent, the active form of **1**:Cu(II):($^{-}OCH_3$) is generated at a relatively low $^{s}_{s}$pH ($^{s}_{s}pK_a$ ≈ 6 or lower as found here), thereby spontaneously forming an appreciable amount of the active form in methanol without adding additional base. In fact, Ni(II) is more catalytically active when fully present as **1**:Ni(II):($^{-}OCH_3$) than is **1**:Cu(II):($^{-}OCH_3$). At a $^{s}_{s}$pH of 10.5, well below the $^{s}_{s}pK_a$ for the ionization of the **1**:Ni(II)-coordinated methanol, the maximum observed rate constant for the Ni(II)-catalyzed cleavage of **1** (k_{obs} ≈ 0.07 s^{-1} at 4 mM Ni(II), not saturating conditions) is 12 times larger than the Cu(II)-catalyzed process (k_{obs} ≈ 0.0057 s^{-1}, under saturation conditions). At higher $^{s}_{s}$pH, and with full binding of the metal ion−methoxide to **1**, the k_{max} for the Ni(II)-promoted reaction would be far greater.

dx.doi.org/10.1021/ic4028755 | Inorg. Chem. 2014, 53, 2211−2221

Table 1. Second-Order Rate Constants for Attack of Alkoxide on the Fully-Formed Substrate:M(II) Complex under Saturation Conditions with Respect to $[M^{2+}]$, Maximal Rate Constants for Selected Substrate:M(II):($^-$OR) complexes at 25 °C

subst.	solvent	Ni k_2^{-OR} (M^{-1} s^{-1})	Zn k_2^{-OR} (M^{-1} s^{-1})	k_{max}^{Zn} (s^{-1})	Cu k_2^{-OR} (M^{-1} s^{-1})	k_{max}^{Cu} (s^{-1})
1	MeOH	*a* $k_3 = 4.4 \times 10^7$ M^{-2} s^{-1} [b]	*a* $k_3 = 4.5 \times 10^6$ M^{-2} s^{-1} [b]	*a*	5.4×10^8	5.7×10^{-3} [d]
	EtOH	1.0×10^{10}	1.7×10^9	*a*	4.5×10^{11}	9.0×10^{-3} [e]
2	MeOH	6.3×10^5	1.5×10^5	5.8×10^{-4} [c]	7.6×10^7	8.0×10^{-4} [f]
	EtOH	7.3×10^9	9.5×10^7	*a*	1.9×10^{10}	3.8×10^{-4} [f]

[a] K_b constants are not available due to the fact that saturation is not observed in the k_{obs} vs $[M^{2+}]$ plots or the k_{obs}^{max} vs $_s^s$pH plots. [b] k_3 is a third-order rate constant calculated for the hypothetical process involving substrate + M^{2+} + $^-$OR. [c] Kinetic $_s^s pK_a$ 8.36. [d] Kinetic $_s^s pK_a$ 5.79. [e] Kinetic $_s^s pK_a$ 5.4. [f] No observed kinetic $_s^s pK_a$.

4.2. Ni(II)- and Zn(II)-Promoted Ethanolysis of 1. The mechanism given in Scheme 1 is also favored for the Ni(II)- and Zn(II)-promoted ethanolysis of **1**. Because of the lower polarity of the medium, their binding to **1** in ethanol is stronger than it is in methanol, leading to saturation of the k_{obs} versus $[M^{2+}]$ plots (see Figure 3). The binding constants for Ni(II) to **1** in ethanol are consistently larger than those for Zn(II), which correlates with the aforementioned trends in binding constants for metal ion−pyridine complexes in water. From the data in Figures 9S and 11S in the Supporting Information, one sees that the k_{obs}^{max} values for the Ni(II) and Zn(II) complexes of **1** at respective $_s^s$pH values of 7.9 and 7.2 are 0.05 s^{-1} and 2.6×10^{-3} s^{-1}. Because these $_s^s$pH values are below the $_s^s pK_a$ for formation of their maximally active **1**:M(II):($^-$OEt) forms, both reactions would be faster at higher $_s^s$pH and indeed faster than the reaction of **1**:Cu(II):($^-$OEt) in ethanol, $k_{max}^{Cu} = 9 \times 10^{-3}$ s^{-1}.

4.3. Cu(II)-Promoted Methanolysis and Ethanolysis of 1. The $_s^s$pH/log(k_{obs}^{corr}) profile for the Cu(II)-promoted methanolysis of **1** from our previous study was extended to determine a kinetic $_s^s pK_a$ of 5.79. This is lower than the value of 6.5 observed for the analogous *N*,*N*-bis(2-picolyl)acetamide-copper(II) complex and may be attributed to a greater stabilization of the conjugate base originating from the more electron-withdrawing *p*-nitrobenzoyl group relative to the acetyl group. The kinetic studies were also carried out in ethanol, where the cleavage reaction has a similar dependence on $_s^s$pH as in methanol. The kinetic $_s^s pK_a$ in ethanol is 5.4, beyond which the k_{max}^{Cu} is 9×10^{-3} s^{-1} (1.5-fold larger than in methanol, 5 times less reactive than the Ni(II) complex in ethanol at $_s^s$pH 7.9, and 3−4 times more reactive than the Zn(II) complex at $_s^s$pH 7.2 in ethanol).

4.4. Ni(II)- and Zn(II)-Promoted Methanolysis of *N*,*N*-Bis((1H-benzimidazol-2-yl)methyl)-*p*-nitrobenzamide (2). The onset of saturation of k_{obs} with increasing $[M^{2+}]$ for the cleavage of **2** indicates that it binds Ni(II) and Zn(II) stronger than does **1** in methanol. The stability constants for the 1:1 complexes formed between Ni^{2+} or Zn^{2+} and benzimidazole in water at 25 °C and μ = 0.5 ($NaNO_3$) are 100 M^{-1} and 41 M^{-1},[34] values larger than those found for the their monopyridine complexes, which mirrors the larger binding constants observed for M(II) complexes of **2** relative to **1**. A somewhat contrasting trend is seen in the order of binding strength of **2** to Zn(II) being slightly stronger than Ni(II) when compared to the values reported for benzimidazole.[34] This discrepancy may be attributable to the differences in the preferred geometry of each metal ion on complexation with polydentate ligands. A distinct characteristic of the **2**:Zn(II) system is the $_s^s$pH independence of k_{obs}^{max} beyond its kinetic $_s^s pK_a$ of 8.36, representing a plateau region with a k_{max} of 5.8×10^{-4} s^{-1} (Figure 16S, Supporting Information).

4.5. Ni(II)- and Zn(II)-Promoted Ethanolysis of 2. The binding constants between Ni^{2+} or Zn^{2+} and **2** in ethanol are larger than those observed with **1** in ethanol. It is noteworthy that **2** appears to bind Zn^{2+} more tightly than Ni^{2+} in ethanol, the opposite of what is seen with **1**, but parallel to the trend observed in methanol. In each case, plots of log(k_{obs}^{max}) versus $_s^s$pH do not show evidence of complete formation of **2**:M(II):($^-$OEt), the highest values attained for the respective Ni(II) and Zn(II) complexes being 0.3 s^{-1} ($_s^s$pH 8.7) and 2.3×10^{-4} s^{-1} ($_s^s$pH 7.5) (see Figures 19S and 21S, Supporting Information).

4.6. Cu(II)-Promoted Methanolysis and Ethanolysis of 2. The k_{max} value for Cu(II)-mediated cleavage of **2** in methanol is about twice that in ethanol ($(3.8 \pm 0.2) \times 10^{-4}$ s^{-1}), the opposite of what is observed in the case of **1**. These values are almost an order of magnitude smaller than those observed for **1** in the corresponding solvents, suggesting a less desirable proximity or more severe restriction of access of the metal-bound ethoxide in the transition state for attack on the C═O unit of the Cu(II)-complex of **2**.

4.7. Comparison of Relative Activity. A convenient way to compare the relative activities of most of the systems considered here assesses the apparent second-order rate constant for the attack of alkoxide (k_2^{-OR}) on the fully formed substrate:M(II) complex as defined in eq 2. These are shown in Table 1 along with other k_{max} values, which have been determined in various ways. The binding of Cu^{2+} with **2** in methanol and ethanol is sufficiently strong that only a value of the maximum unimolecular rate constant k_{max}^{M} for decomposition of the substrate:Cu(II):($^-$OR) complex at three different $_s^s$pH values could be obtained. In theory, complete plots of the log(k_{max}^{obs}) values versus $_s^s$pH will show linear behavior with a gradient of unity at values below the $_s^s pK_a$ for formation of the substrate:M(II):($^-$OR) complex and a plateau with a zero gradient at greater $_s^s$pH values. The latter behavior with respect to increasing $_s^s$pH was only realized with Cu^{2+} and **1** in methanol and ethanol and with Zn^{2+} and **2** in methanol. A complete analysis through NLLSQ fitting of the log(k_{max}^{obs}) versus $_s^s$pH values to eq 1 yields first-order rate constants (k_{max}^{M}) for decomposition of the maximally active substrate:M(II):($^-$OR) form and their kinetic $_s^s pK_a$ values, which are given in Table 1. Plots of k_{obs} versus $[M^{2+}]$ show saturation for Cu^{2+}, Zn^{2+}, and Ni^{2+} with **1** in ethanol, Cu^{2+} with **1** in methanol, and Zn^{2+} and Ni^{2+} with **2** in methanol and ethanol, which allows us to obtain the k_{obs}^{max} rate constant for reaction of the substrate:M(II) complex at each experimentally attainable $_s^s$pH. For these examples, which do not show a saturation in the log(k_{obs}^{max}) versus $_s^s$pH plots (due to the fact that the experimentally accessible $_s^s$pH values are less than the $_s^s pK_a$), one can obtain the apparent k_2^{OR} rate constant for $^-$OR attack on

dx.doi.org/10.1021/ic4028755 | Inorg. Chem. 2014, 53, 2211−2221

the substrate:M(II) complex by averaging the individual k_2^{-OR} values at each [$^-$OR].[35]

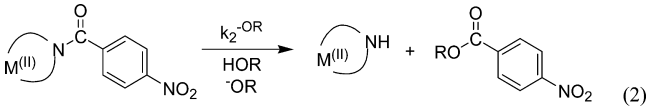

The M k_2^{-OR} constants given in Table 1 are large for all complexes in both solvents, and in some cases approach, and even exceed, the diffusion limit in methanol ($1-2 \times 10^{10}$ M^{-1} s^{-1})[36] and ethanol (2×10^{10} M^{-1} s^{-1}).[37] The fact that the k_2^{-OR} value for **1**:Cu(II) in ethanol (4.5×10^{11} M^{-1} s^{-1}) is computed to exceed the diffusion limit in that solvent by ~20 times can be taken as confirmation that the true reaction does not involve the attack of external ethoxide on **1**:Cu(II), but rather decomposition of a **1**:Cu(II):($^-$OEt) complex. By extension, it seems reasonable to propose that all of these reactions occur through the metal-bound lyoxide form, as proposed previously.[16,17]

4.8. Acceleration of Amide Cleavage Provided by the Presence of a Metal Ion. The acceleration of the alcoholysis of benzamides **1** and **2** provided by the metal ion can be conveniently measured in three ways. The first involves comparing the k_2^{-OR} rate constant for alkoxide attack on the substrate:M(II) complex with that for attack of alkoxide on the uncomplexed **1** or **2**. Previously[17] we experimentally determined that the methoxide-promoted reaction of 0.15 M **1** in 0.3 M $KOCH_3$ shows no indication of product formation after 52.5 d. We have now extended the time to 250 d without observing product formation. Assuming we could detect 1 mM of the product, the upper limit for the second-order rate constant is $k^{-OMe1} = 1 \times 10^{-9}$ M^{-1} s^{-1}. While we do not have experimental data for the ethanolysis reaction of **1**, Phan and Mayr have reported that the k^{-OMe} values for nucleophilic addition of methoxide in methanol to trinitrotoluene or benzhydrilium ions are 5 times less than the nucleophilic addition of ethoxide in ethanol.[38] In another comparison, methoxide attack on *p*-nitrophenyl acetate in methanol is reported[39a] to be essentially the same as the attack of ethoxide in ethanol.[39b] If we are allowed to use these comparisons, then the approximate upper limit for the k_2^{-OEt} reaction with **1** is ~1×10^{-9} M^{-1} s^{-1}. Unfortunately experimental data corresponding to the alkoxide reactions of **2** are not obtainable due to technical problems of deprotonation of the benzimidazole N–H under strongly basic conditions.

The second methodology involves comparing the first-order rate constant observed for decomposition of substrate:M(II):(HOR) at the $_s^spK_a$ for its acid dissociation, with the pseudo-first-order rate constant that would be observed for alkoxide attack on substrate at a $_s^spH$ corresponding to that $_s^spK_a$. Using the above comparisons, the accelerations in methanol and ethanol for the various complexes of **1** compared with the background methoxide reactions are given in Table 2.

A third and more informative method for judging the efficacy of the metal ion-promoted reaction compares the ΔG^o of binding of the metal ion to the transition state of the presumed lyoxide-promoted reaction, namely, [S:M(II):($^-$OR)]‡ with that of the lyoxide reaction, [S:($^-$OR)]‡.[40,41] The thermodynamic cycle is shown in Scheme 2, where M(II) is represented as M and the various free energies for the kinetic and equilibrium terms can be obtained from the rate constants for attack of alkoxide on the substrate or its metal-complexed form (k_2^{-OR} and Mk_2^{-OR}) and the metal binding constants (K_b).

Table 2. Acceleration of Amide 1 Alcoholysis Provided by the Presence of a Divalent Metal Ion at 25 °C

benzamide	solvent	Ni(II)	Zn(II)	Cu(II)
1	MeOH	$(1.3 \times 10^{14})^a$	$(4.9 \times 10^{13})^b$	$(3.5 \times 10^{17})^c$ $(3 \times 10^{17})^d$
	EtOH	$(1.7 \times 10^{18})^e$	$(2.5 \times 10^{17})^e$	$(9 \times 10^{18})^f$

[a]Computed from k_{obs} value for decomposition of **1**:Ni(II) at $_s^spH$ 10.5 (k_{obs} = 0.07 s^{-1} at 4 mM Ni(II), not saturating conditions). This provides a lower limit for the acceleration since the Ni(II) complex is not fully formed. [b]Computed from k_{obs} value for decomposition of **1**:Zn(II) at $_s^spH$ 9.6 (k_{obs} = 3.3×10^{-4} s^{-1} at 1 mM Zn(II), not saturating conditions). This provides a lower limit for the acceleration since the Zn(II) complex is not fully formed. [c]Computed from comparison of the k_2^{-OMe} value for attack of methoxide on **1**:Cu(II) given in Table 1 with the second-order rate constant for attack of methoxide on **1**. [d]Computed from comparison of the first-order rate constant for decomposition of **1**:Cu(II):($HOCH_3$) at $_s^spH$ 5.79, corresponding to the kinetic $_s^spK_a$, with the pseudo first-order rate constant for reaction of methoxide with **1** at that $_s^spH$. [e]Computed from the k_2^{-OEt} values for the Ni(II) and Zn(II) complexes of **1** from Table 1 compared with the second-order rate constant for attack of ethoxide on **1**. [f]Computed from comparison of the first-order rate constant for decomposition of **1**:Cu(II):(HOEt) at $_s^spH$ 5.4, corresponding to the kinetic $_s^spK_a$ in ethanol, with the pseudo first-order rate constant for reaction of ethoxide with **1** at that $_s^spH$.

Scheme 2. A Thermodynamic Cycle Describing the Free Energies for Various Equilibrium and Kinetic Steps for Alkoxide Attack on Substrate S, Equilibrium Binding of the Metal Ion to S, and Alkoxide Attack on the S:M Complex (Metal Ion Charges Omitted for Clarity). Products Include the Dipicolyl Amine and Dibenzimidazol-2-ylmethyl Amine Ligands

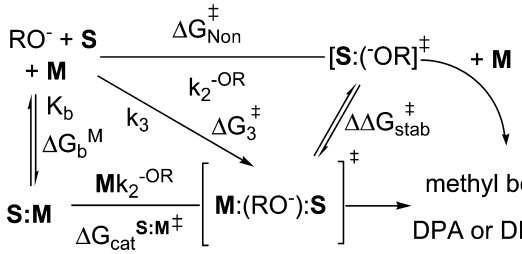

$\Delta\Delta G^‡_{stab}$ is computed from the expression given in eq 3, which is applicable for the situations where Ni, Zn, and Cu bind with saturation to the substrate in ethanol.

$$\Delta\Delta G^‡_{stab} = (\Delta G^M_b + \Delta G^{S:M‡}_{cat}) - \Delta G^‡_{non} = -RT\ln\left[\frac{(k_2)(K_b)}{k_2^{-OR}}\right] \quad (3)$$

For the situation where no saturation binding of the metal ion to the substrate is observed, in the cases of Zn and Ni in methanol, the hypothetical third-order rate constant (k_3) for reaction of substrate + M(II) + $^-$OR was computed,[42] and the $\Delta\Delta G^‡_{stab}$ is obtained from the expression given in eq 4.

$$\Delta\Delta G^‡_{stab} = \Delta G^‡_3 - \Delta G^‡_{non} = -RT\ln\left[\frac{k_3}{k_2^{-OR}}\right] \quad (4)$$

The results at a standard state of 1 M and 298 K are shown graphically in Figure 9, using the value of 1×10^{-9} M^{-1} s^{-1} as the upper limit for attack of methoxide or ethoxide on substrate **1** in methanol or ethanol in the absence of catalytic metal ion.

dx.doi.org/10.1021/ic4028755 | Inorg. Chem. 2014, 53, 2211–2221

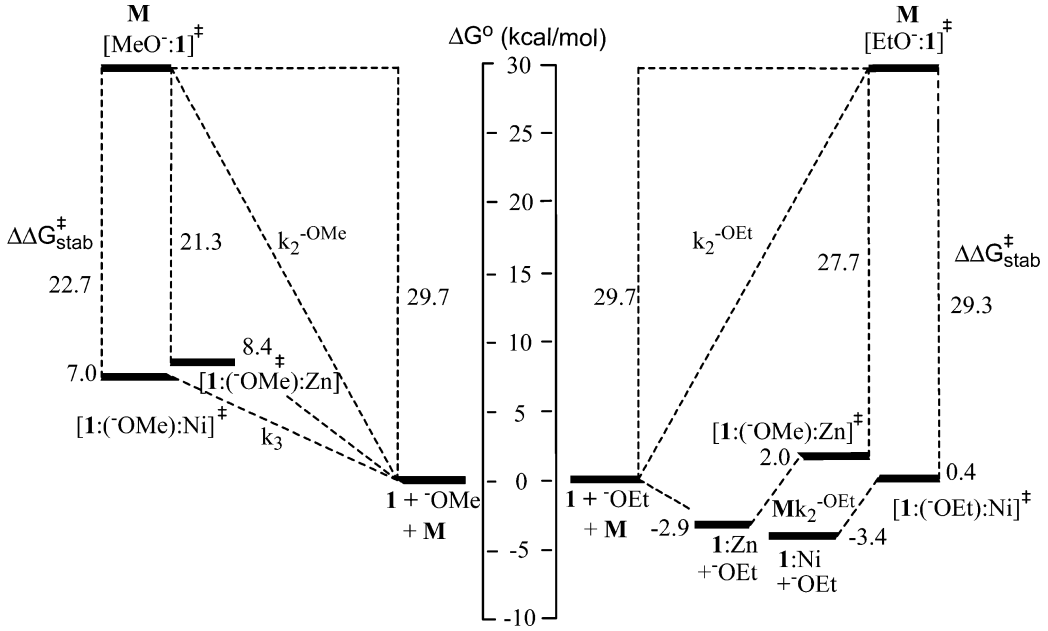

Figure 9. A free-energy diagram obtained for the alcoholysis of **1** in the presence of methoxide in methanol (left side) and ethoxide in ethanol (right side), and in the presence of Zn and Ni in both solvents at standard state. The computed stabilizations of the [lyoxide:**1**]‡ by its binding to the metal ions, $\Delta\Delta G^{\ddagger}_{stab}$ are given numerically on the extreme left and right sides of the diagram and are computed as described in the text.

On the right side of the diagram are included the numerical values obtained for the process in ethanol where metal binding to **1** is sufficiently strong to obtain K_b and a ΔG^{M}_{b}. It is of interest to note that the $\Delta G^{1:M\ddagger}_{cat}$ values obtained from the large Mk_2^{-OEt} values in Table 1 nearly offset the ΔG^{M}_{b} values such that the $[\mathbf{1}:^{-}OEt:M]^{\ddagger}$ transition states lie very close in energy to the free energy of the nonassociated substrate, metal ion, and alkoxide partners. This illustrates that, once the metal ion binds the ethoxide and substrate, their transition states for reaction are stabilized by 27.7 and 29.3 kcal/mol for Zn and Ni, respectively. For these two metal ions in methanol, the transition state binding is not as large, being 21.3 and 22.7 kcal/mol for Zn and Ni. That this is less than in ethanol is a consequence of the reduced affinity of the metal ion for the substrate and methoxide binding in the ground state, which is more largely manifested in binding the transition state although less so than in ethanol. This sort of effect is reminiscent of a dinuclear Zn(II) catalyst that promotes the methanolytic and ethanolytic cleavage of phosphate diesters where extremely large binding of the catalyst to the [alkoxide:substrate] transition states leads to very large rate accelerations.[41d]

5.0. CONCLUSIONS

The results of this study in combination with related ones[12−17] have established that large accelerations for amide cleavage reactions over background base-promoted reactions can be achieved by the multifunctional role of a single metal ion that is appropriately positioned relative to the >N−C═O moiety. To fully realize these effects in small molecules requires a substrate design where the metal ion is forced into binding the lone pair of the amidic N, concurrently positioning a metal-bound nucleophile in a favorable trajectory for attack on the acyl group, with subsequent assistance of the departure of the LG anion. In an optimized system, the metal ion seems to enact several catalytic roles such as was seen earlier in the methanolytic cleavage of a thiobenzanilide catalyzed by a simple palladacycle catalyst.[43] In that case, the Pd enhances the electrophilicity of the thioamide through favorable binding of the C═S unit and delivers the activated methoxide nucleophile to form a tetrahedral intermediate, which subsequently rearranges to allow assisted leaving group departure through Pd−N-coordination. That this sort of trifunctional role for three other transition metal ions is seen to provide catalytic accelerations of 10^{14} to 10^{19} in the present systems dealing with alcoholysis of benzamides **1** and **2** may imply that metal ion assistance of leaving group departure plays a key role that may also be operative in metallo-enzyme promoted cleavage of peptides.

■ ASSOCIATED CONTENT

Ⓢ Supporting Information

Experimental protocol for kinetics, NMR spectral data for **2**, plots of rate constant versus metal ion concentration or $_{s}^{s}$pH, tables of rate constants for metal ion-catalyzed reactions of **1** and **2**, 43 pages. This material is available free of charge via the Internet at http://pubs.acs.org.

■ AUTHOR INFORMATION

Corresponding Author

*Email: rsbrown@chem.queensu.ca. Phone: 613-533-2400. Fax: 613-533-6669.

Notes

The authors declare no competing financial interest.

■ ACKNOWLEDGMENTS

The authors gratefully acknowledge the generous support of the Natural Sciences and Engineering Research Council of Canada (NSERC) and Queen's University. In addition, M.A.R.R. thanks the Government of Ontario and Queen's University for a QEII-GSST. L.C. also thanks the Government of Ontario and Queen's University for the award of a 2012 Summer Work Experience Program (SWEP) stipend. Finally, the authors gratefully acknowledge the assistance of Ms. Aurora

Antoft-Finch who assisted in the collection of a portion of the kinetic data presented in this report.

REFERENCES

(1) (a) Brown, R. S.; Neverov, A. A. *J. Chem. Soc., Perkin Trans. 2* **2002**, 1039. (b) Brown, R. S.; Neverov, A. A.; Tsang, J. S. W.; Gibson, G. T. T.; Montoya-Peláez, P. J. *Can. J. Chem.* **2004**, *82*, 1791. (c) Brown, R. S.; Neverov, A. A. *Adv. Phys. Org. Chem.* **2008**, *42*, 271. (d) Brown, R. S.; Lu, Z.-L.; Liu, C. T.; Tsang, W. Y.; Edwards, D. R.; Neverov, A. A. *J. Phys. Org. Chem.* **2009**, *23*, 1. and references therein (e) Brown, R. S. In *Progress in Inorganic Chemistry;* Karlin, K., Ed.; John Wiley and Sons: Hoboken, NJ, 2011, *57*, 55 and references therein.

(2) (a) Williams, N. H.; Takasaki, B.; Wall, M.; Chin, J. *Acc. Chem. Res.* **1999**, *32*, 485. (b) Morrow, J. *Comments Inorg. Chem.* **2008**, *29*, 169. (c) Fothergill, M.; Goodman, M. F.; Petruska, J.; Warshel, A. *J. Am. Chem. Soc.* **1995**, *117*, 11619. (d) Richard, J. P.; Amyes, T. L. *Bioorg. Chem.* **2004**, *32*, 354.

(3) (a) Liu, C. T.; Neverov, A. A.; Maxwell, C. I.; Brown, R. S. *J. Am. Chem. Soc.* **2010**, *132*, 3561. (b) Raycroft, M. A. R.; Liu, C. T.; Brown, R. S. *Inorg. Chem.* **2012**, *51*, 3846.

(4) Brown, R. S.; Bennet, A. J.; Slebocka-Tilk, H. *Acc. Chem. Res.* **1992**, *25*, 481.

(5) (a) Kester, W. R.; Matthews, B. W. *Biochemistry* **1977**, *16*, 2506. (b) Matthews, B. W. *Acc. Chem. Res.* **1988**, *21*, 333. (c) Pelmenschikov, V.; Blomberg, M. R. A.; Siegbahn, P. E. M. *J. Biol. Inorg. Chem.* **2002**, *7*, 284.

(6) Rawlings, N. D.; Barrett, A. J. Introduction: metallopeptidases and their clans. In *Handbook of Proteolytic Enzymes,* 2nd ed.; Barrett, A. J.; Rawlings, N. D.; Woessner, J. F., Eds.; 2004, *1*, 231.

(7) Balasubramanian, A.; Ponnuraj, K. *J. Mol. Biol.* **2010**, *400*, 274.

(8) Fukasawa, K. M.; Hata, T.; Ono, Y.; Hirose, J. *J. Amino Acids.* DOI: 10.4061/2011/574816. Published Online: **2011**.

(9) (a) Polzin, G. M.; Burstyn, J. N. *Met. Ions in Biol. Syst.* **2000**, *38*, 103. (b) Fife, T. H.; Bembi, R. *J. Am. Chem. Soc.* **1994**, *115*, 11358. (c) Schepartz, A.; Breslow, R. *J. Am. Chem. Soc.* **1987**, *109*, 1814. (d) Suh, J.; Moon, S.-J. *Inorg. Chem.* **2001**, *40*, 4890. (e) Neverov, A. A.; Montoya-Peláez, P. J.; Brown, R. S. *J. Am. Chem. Soc.* **2001**, *123*, 210. (f) Neverov, A. A.; Brown, R. S. *Can. J. Chem.* **2000**, *78*, 1247 and references therein.

(10) Liu, C. T.; Maxwell, C. I.; Pipe, S. G.; Neverov, A. A.; Mosey, N. J.; Brown, R. S. *J. Am. Chem. Soc.* **2011**, *133*, 20068.

(11) Elton, E. S.; Zhang, T.; Prabhakar, R.; Anif, A. M.; Berreau, L. M. *Inorg. Chem.* **2013**, *52*, 11480 and references therein.

(12) Houghton, R. P.; Puttner, R. R. *Chem. Commun.* **1970**, 1270.

(13) Niklas, N.; Heinemann, F. W.; Hampel, F.; Clark, T.; Alsfasser, R. *Inorg. Chem.* **2004**, *43*, 4663 and references therein.

(14) Niklas, N.; Alsfasser, R. *Dalton Trans.* **2006**, 3188.

(15) (a) Bröhmer, M. C.; Bannwarth, W. *Eur. J. Org. Chem.* **2008**, 4412. (b) Bröhmer, M. C.; Mundinger, S.; Bräse, S.; Bannwarth, W. *Angew. Chem., Int. Ed.* **2011**, *50*, 6125.

(16) Barrera, I. F.; Maxwell, C. I.; Neverov, A. A.; Brown, R. S. *J. Org. Chem.* **2012**, *77*, 4156.

(17) Raycroft, M. A. R.; Maxwell, C. I.; Oldham, R. A. A.; Saffouri Andrea, A.; Neverov, A. A.; Brown, R. S. *Inorg. Chem.* **2012**, *51*, 10325.

(18) For the designation of pH in nonaqueous solvents we use the nomenclature recommended by the IUPAC: *Compendium of Analytical Nomenclature. Definitive Rules 1997*, 3rd ed.; Blackwell: Oxford, U. K., 1998. The pH meter reading for an aqueous solution determined with an electrode calibrated with aqueous buffers is designated as ${}^{w}_{w}$pH; if the electrode is calibrated in water and the "pH" of the neat buffered alcohol solution is then measured, the term ${}^{s}_{w}$pH is used; and if the electrode is calibrated in the same solvent in which the "pH" reading is made, then the term ${}^{s}_{s}$pH is used. In methanol, ${}^{s}_{s}\mathrm{pH} = {}^{s}_{w}\mathrm{pH} - (-2.24)$, and since the autoprotolysis constant of methanol is $10^{-16.77}$ M^2, neutral ${}^{s}_{s}$pH is 8.4. In ethanol, ${}^{s}_{s}\mathrm{pH} = {}^{s}_{w}\mathrm{pH} - (-2.54)$, and since the autoprotolysis constant of ethanol is $10^{-19.1}$ M^2, the neutral ${}^{s}_{s}$pH is 9.6.

(19) Siddiqi, Z. A.; Kumar, S.; Khalid, M.; Shahid, M. *Spectrochim. Acta, Part A* **2009**, *71*, 1845.

(20) (a) Gibson, G.; Neverov, A. A.; Brown, R. S. *Can. J. Chem.* **2003**, *81*, 495. (b) Gibson, G. T. T.; Mohamed, M. F.; Neverov, A. A.; Brown, R. S. *Inorg. Chem.* **2006**, *45*, 7891.

(21) Li, C.; Tian, H.; Duan, S.; Liu, X.; Xu, P.; Qiao, R.; Zhao, Y. *J. Phys. Chem. B* **2011**, *115*, 13350.

(22) Gibson, G. T. T. *Metal Ion Speciation in Methanol and Ethanol Determined by Potentiometric Titration and its Relevance to Metal Ion-Catalyzed Alcoholysis Reactions.* Ph.D. Dissertation, Queen's University, Kingston, Ontario, Canada, 2006.

(23) Liu, C. T.; Neverov, A. A.; Brown, R. S. *J. Am. Chem. Soc.* **2008**, *130*, 1671.

(24) Harned, H. S.; Owen, B. B. *The Physical Chemistry of Electrolytic Solution;* ACS Monograph Series 137, 3rd ed.; Reinhold Publishing: New York, 1957, p 161.

(25) (a) ${}^{s}_{s}$pH values in ethanol were determined as discussed in references 18 and 20. (b) The first macroscopic ${}^{s}_{s}pK_a$ of Ni(II)-coordinated ethanol is 8.65 as determined by a half-neutralization experiment at $[Ni(ClO_4)_2]$ = 1 mM; the second macroscopic ${}^{s}_{s}pK_a$ is 8.95. Such a steep titration profile indicates strong correlation between first and second dissociation steps, possibly due to a dimerization or oligomerization process involving M(II):($^{-}$OR) as has been previously observed for some metal ions in methanol and ethanol (reference 20).

(26) It has been previously observed that, in the case of Zn^{2+} ions, binding of the second ligand tends to be stronger than the first. For example, the sequential binding constants of chloride anions to Zn^{2+} in methanol are equal to $K_1 = 7.76 \times 10^3$ M^{-1} and $K_2 = 1.71 \times 10^4$ M^{-1}.[27] This cooperative effect is often thought to be a consequence of the change in coordination sphere as a result of binding the first ligand.

(27) Doe, H.; Kitagawa, T. K. *Inorg. Chem.* **1982**, *21*, 2272.

(28) In the low ${}^{s}_{s}$pH domain of the log(k_2) plot, the data begin to curve downward (lowest ${}^{s}_{s}$pH datum omitted), which may be indicative of weakened binding between Ni^{2+} and compound **2** due to the onset of competitive protonation of the benzimidazole nitrogens. This process, however, does not appear to affect the overall activity of the complex (k_{max}).

(29) In the case of strong interactions between the metal ion and substrate, the determination of the binding constant is inherently difficult, and often only a lower limit can be defined with any certainty.

(30) IUPAC. *Compendium of Chemical Terminology, 2nd ed. (the "Gold Book"),* Compiled by A. D. McNaught and A. Wilkinson. Blackwell Scientific Publications, Oxford, **1997**. XML on-line corrected version: http://goldbook.iupac.org 2006—created by Nic, M.; Jirat, J.; Kosata, B.; updates compiled by A. Jenkins. ISBN 0967855098. DOI:10.1351/goldbook.

(31) While intermolecular and intramolecular attack of methoxide are kinetically indistinguishable processes, the latter process is most likely based on the results with the Cu(II) complex.

(32) Rabinovich, V. A.; Khavin, Z. *Concise Handbook of Chemistry*; Khimiya: Leningrad, 1977 [in Russian].

(33) Kapinos, L. E.; Sigel, H. *Inorg. Chim. Acta* **2002**, *337*, 131.

(34) Kapinos, L. E.; Song, B.; Sigel, H. *Chem.—Eur. J.* **1999**, *5*, 1794.

(35) The apparent k_2^{-OR} rate constant for attack of alkoxide on the M(II) complex of **1** or **2** is given as $k_2 = k^{obs}_{max}\,({}^{s}_{s}K_a/({}^{s}_{s}K_a + [H^+]))$[16,17]. Under conditions where ${}^{s}_{s}K_a < [H^+]$ the reaction is first order in [$^{-}$OR] since $k_2 = k^{obs\,s}_{maxs}K_a/[H^+] = k^{obs}_{max}\,({}^{s}_{s}K_a/(K_{auto}))[^{-}OCH_3]$. Given ${}^{s}_{s}pK_a$ values of 5.79 for formation of **1**:Cu(II):($^{-}$OCH$_3$), and 8.36 for formation of **2**:Zn(II):($^{-}$OCH$_3$) and an autoprotolysis constant for methanol of $K_{auto} = 10^{-16.77}$ M^2, one computes that $k_2^{1:Cu(II)} = 5.7 \times 10^8$ M^{-1} s^{-1}, while $k_2^{2:Zn(II)}$ is 1.5×10^5 M^{-1} s^{-1}.

(36) (a) Bachviser, S. F; Gehlen, M. H. *J. Chem. Soc., Faraday Trans.* **1997**, *93*, 1133. (b) Zanini, G. P.; Montejano, H. A.; Previtali, C. M. *J. Chem. Soc., Faraday Trans.* **1995**, *91*, 1197. (c) Marshall, D. B.; Eyring, H. M.; Strohbusch, F.; White, R. D. *J. Am. Chem. Soc.* **1980**, *102*, 7065.

(37) Schwartz, H. A.; Gill, P. S. *J. Chem. Phys.* **1977**, *81*, 22.

(38) Phan, T. B.; Mayr, H. *Can. J. Chem.* **2005**, *83*, 1554.

(39) (a) Schowen, R. L; Behn, G. C. *J. Am. Chem. Soc.* **1968**, *90*, 5839, (220 ± 100 M^{-1} s^{-1}, 27.2 °C). (b) Guanti, G.; Cevasco, G.; Thea, S.; Dell'Erba, C.; Petrillo, G. *J. Chem. Soc., Perkin Trans. 2* **1981**, 327, (107 ± 2 M^{-1} s^{-1}, 22 °C).

(40) Wolfenden, R. *Nature* **1969**, *223*, 704.
(41) For applications of this to phosphate cleavage and other reactions see (a) Yatsimirsky, A. K. *Coord. Chem. Rev.* **2005**, *249*, 1997. and references therein. (b) Iranzo, O.; Kovalevsky, A. Y.; Morrow, J. R.; Richard, J. P. *J. Am. Chem. Soc.* **2003**, *125*, 1988. (c) Bunn, S. E.; Liu, C. T.; Lu, Z.-L.; Neverov, A. A.; Brown, R. S. *J. Am. Chem. Soc.* **2007**, *129*, 16239. (d) Liu, C. T.; Neverov, A. A.; Brown, R. S. *J. Am. Chem. Soc.* **2008**, *130*, 16711.
(42) While the actual reaction must proceed through the bound form of **S**:M(II):($^{-}$OR), the experimental kinetic regime did not allow us to determine the actual binding constants for this species. Hence, for the purposes of determining the energetics associated with the process described in Scheme 2, the third-order rate constant was determined as the average of the second-order rate constant for metal dependence at each pH divided by the [$^{-}$OR].
(43) Liu, C. T.; Maxwell, C. I.; Pipe, S. G.; Neverov, A. A.; Mosey, N. J.; Brown, R. S. *J. Am. Chem. Soc.* **2011**, *133*, 20068.

dx.doi.org/10.1021/ic4028755 | *Inorg. Chem.* 2014, 53, 2211−2221